

Least-squares Kirchhoff Imaging with a Simplified PSF Formula

C. Zhou¹, N. Chemingui¹, Y. He¹, J. Brittan¹

¹ TGS

Summary

Least-squares imaging in image domain utilizes Point Spread Functions (PSFs) to estimate the Hessian matrix. The conventional way to compute PSFs involves cascaded operations -modelling followed by migration. In this paper, we propose a least-squares Kirchhoff imaging method in which the PSFs are computed explicitly with a simplified formula and then reshaped with the Kirchhoff image. A preconditioned iterative conjugate solver is chosen for the inversion as the final step of the least-squares imaging. The field example demonstrates the improvements in image resolution and clarity with the proposed method.

Introduction

Least-squares Kirchhoff imaging remains essential as it provides a robust and effective method for reconstructing high-resolution subsurface images from seismic data, particularly in complex geological environments. Image-domain least-squares imaging often utilizes Point Spread Functions (PSF) to compute the Hessian matrix, which is applied to deblur the conventional migrated image (e.g., Schuster and Hu, 2000). This process typically involves a cascaded application of modeling and migration. The standard seismic image, m_0 , is generated by depth migrating the acquired seismic data:

$$m_0 = L^T d = L^T L m, \quad (1)$$

where d is the seismic data, L^T is the migration operator, m is the reflectivity model of the earth and $H = L^T L$ is the Hessian matrix.

Since the Hessian matrix is not unitary, the migrated image represents a blurred version of the true reflectivity rather than the reflectivity itself. Image-domain least-squares imaging addresses this by solving for the true reflectivity, m , using the following linear equation:

$$H m = m_0, \quad (2)$$

where H is typically computed as the Point Spread Function (PSF) by performing the modeling operation followed by the migration operation at discrete locations. (Fletcher *et al.*, 2016).

The computation of the Hessian involves two operations: modeling and migration, which can be computationally expensive. To improve the efficiency of this process, researchers have developed one-operation approaches. For example, Xu *et al.* (2022) derived a PSF formula based on the WKBJ approximation for Least-Squares Reverse Time Migration (LSRTM). Similarly, Lund *et al.* (2022) proposed an analytical PSF computation method for Kirchhoff least-squares imaging. Compared to the conventional method of computing PSFs through a modeling operation followed by a migration operation, these one-operation approaches are significantly more computationally efficient. In this paper, we propose an efficient image-domain least-squares Kirchhoff imaging method. First, we compute PSFs using a simplified true-amplitude Kirchhoff formula. Next, we reshape the wavenumber spectra of the computed PSFs to match the migrated image. Finally, we iteratively invert for the reflectivity using a preconditioned system.

The simplified PSF formula

For a scatterer located at x_c in the subsurface, the seismic signal Ψ , which originates from a source at location x_s , scatters at x_c , and is recorded at a receiver at x_r can be expressed as:

$$\Psi(t) = s(t - (t_s + t_r)) A(x_s, x_c) A(x_c, x_r), \quad (3)$$

where s is the source wavelet, $A(x_s, x_c)$ is the amplitude of the Green's function from the source to the scatterer, $A(x_c, x_r)$ from the scatterer to the receiver, t_s and t_r are the travel-times from the source to the scatterer and from the scatterer to the receiver respectively.

The true amplitude Kirchhoff migration (Albertin *et al.* 1999) is expressed as:

$$r(x) = \sum_i \frac{f_i(x)}{n(v_i)}, \quad (4)$$

$$f_i(x) = -\frac{1}{4\pi^2} \frac{p(x)}{A(x_s, x) A(x, x_r)} \frac{\partial}{\partial t} \Psi * \Delta(t), \quad (5)$$

where $p(x)$ is the slowness at x , n is the hit count in subsurface illumination angle bin v_i and $\Delta(t)$ is the delta function. In the vicinity of the scatterer with $x \approx x_c$, the amplitude of the Green's functions in equation (5) can be approximated with that at x_c and equation (5) becomes:

$$f_i(x) \approx -\frac{1}{4\pi^2} \frac{p(x)}{A(x_s, x_c)A(x_c, x_r)} \frac{\partial}{\partial t} \Psi * \Delta(t). \quad (6)$$

Combining equations (4), (5) and (6) we get the simplified PSF formula:

$$H = -\frac{1}{4\pi^2} \sum_i \frac{p(x)}{n(v_i)} \frac{\partial}{\partial t} s(t - (t_s + t_r)) * \Delta(t). \quad (7)$$

Equation (7) offers an efficient method for computing the PSF directly, eliminating the need for cascaded modeling and migration operations. Lund *et al.* (2022) also developed an explicit Kirchhoff PSF formula, which includes more terms compared to Equation (7).

It is important to note that Equation (7) is derived without making any assumptions about the acquisition geometry. As a result, it can be used to compute PSFs for any type of acquisition, whether land or marine, including streamers or OBN. Furthermore, it does not require any additional processing, such as data regularization, to generate true-amplitude PSFs.

Reshaping the Hessian

While the modeling operation is not required to compute the Kirchhoff PSF, we derive the PSF formula (Equation 7) from the modeling equation (Equation 3). However, like other ray-based algorithms, Equation 3 is unable to accurately model wave propagation in complex earth media. In fact, even with advanced wave equation-based methods, accurately modeling the wavefield remains a challenge.

For instance, as seismic waves propagate through the earth, some of their energy is absorbed or attenuated due to intrinsic and scattering attenuation. Intrinsic attenuation is frequency-dependent, while scattering attenuation depends on both frequency and the size of the scatterers, such as cracks and inclusions in the earth. Techniques like Q tomography and Q compensation (Valenciano and Chemingui, 2013) have been widely used to enhance seismic image quality. Despite these efforts, the spectra of seismic images often vary from shallow to deep regions. One reason for this is the difficulty in obtaining an accurate Q model. Additionally, scattering attenuation is not typically accounted for due to the challenges in estimating it. Finally, even with a precise Q model, seismic signals attenuated below the noise level cannot be recovered. In our approach, we do not include Q in the computation of the Hessian. Therefore, the PSFs computed using equation (7) do not capture the spectral properties of the true Hessian. Including Q in this process may make the computed PSFs closer to the true Hessian, but it will increase the cost. On the other hand, the seismic image contains information that can be injected into the PSFs. Specifically, the wave number spectra in the seismic image can be used to reshape the computed PSFs:

$$H_s = R(H, m_0), \quad (8)$$

where R represents the reshaping operation. The computed PSFs are reshaped in the wavenumber domain and then transformed back to the spatial domain. The rationale is that, if the modeling and migration are done accurately, the computed PSF and the seismic image should have similar wavenumber spectra.

Iterative inversion

The Hessian matrix is symmetric. An iterative conjugate gradient solver is chosen to solve the linear system of equations in (2). Due to the presence of noise, regularization or preconditioning is often applied to the linear system. The application of a preconditioner results in

$$Pm_0 = PH_s m, \quad (9)$$

where P is the preconditioner and H_s is the computed and reshaped Hessian matrix. The preconditioning operation can be as simple as a diagonal scaling (Jacobi preconditioning), though one that incorporates structural information is preferred.

Field example

We applied the proposed least-squares imaging method to a deep-water streamer dataset from the Campos Basin offshore Brazil. The narrow-azimuth streamer acquisition utilized 8 km streamers. PSFs were computed and reshaped for all offsets (Fig. 1). The input Kirchhoff offset gathers were muted to remove refracted and post-critical angle energy. Compared to the Kirchhoff offset gathers (Fig. 2, left), the least-squares gathers (Fig. 2, right) provide higher resolution and a better signal-to-noise ratio. Thin layers that appear with low wavenumber in the Kirchhoff gathers (Fig. 2, left) are more clearly defined in the least-squares gathers (Fig. 2, right). The vertical section of the least-squares image (Fig. 3, middle) offers higher resolution and clearer fault imaging compared to the Kirchhoff image (Fig. 3, left). The least-squares image also yields a broader bandwidth (Fig. 3, right). The depth slice of the least-squares image demonstrates higher horizontal resolution and improved image clarity (Fig. 4, right), overall outperforming the Kirchhoff image (Fig. 4, left).

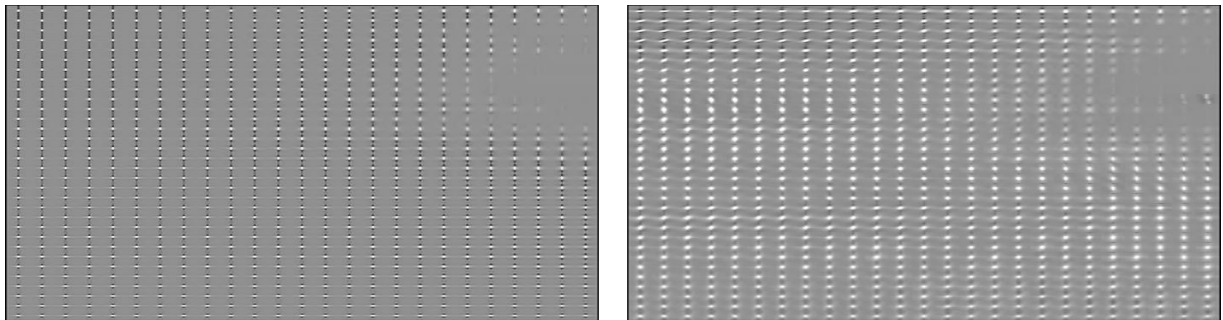


Figure 1 The offset PSF gather computed with equation (7) (left) and the reshaped gather (right) at one common midpoint. The vertical axis is depth, and the horizontal axis is offset.

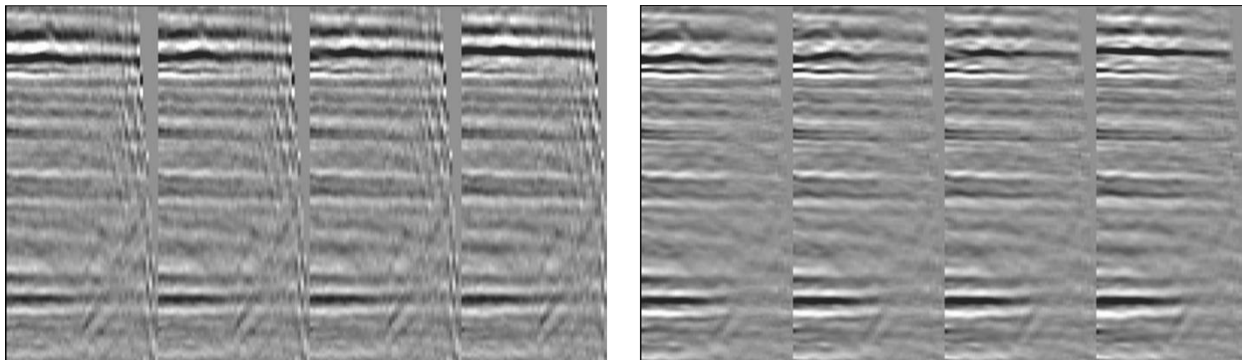


Figure 2 Pre-salt Kirchhoff offset gathers (left) vs. least-squares Kirchhoff gathers (right). The depth range is 6100 -- 8300 m.

Conclusions

In this paper, we derive a simplified formula for computing Kirchhoff PSFs. The simplicity of the formula makes PSF computation cost-effective and applicable to data from any acquisition geometry. The computed PSFs are reshaped using the seismic image's wavenumber spectra, resulting in an accurate Hessian matrix. A preconditioned conjugate gradient solver is employed for the least-squares inversion. The field example demonstrates significant improvements in image resolution and clarity.

Acknowledgements

The authors thank TGS for the permission to publish this work, Colleagues Rachel Collins and Claire Glynn for providing the Kirchhoff seismic gathers and velocity model. Øystein Korsmo, Faqi Liu and Carlos Calderon are also thanked for their constructive suggestions

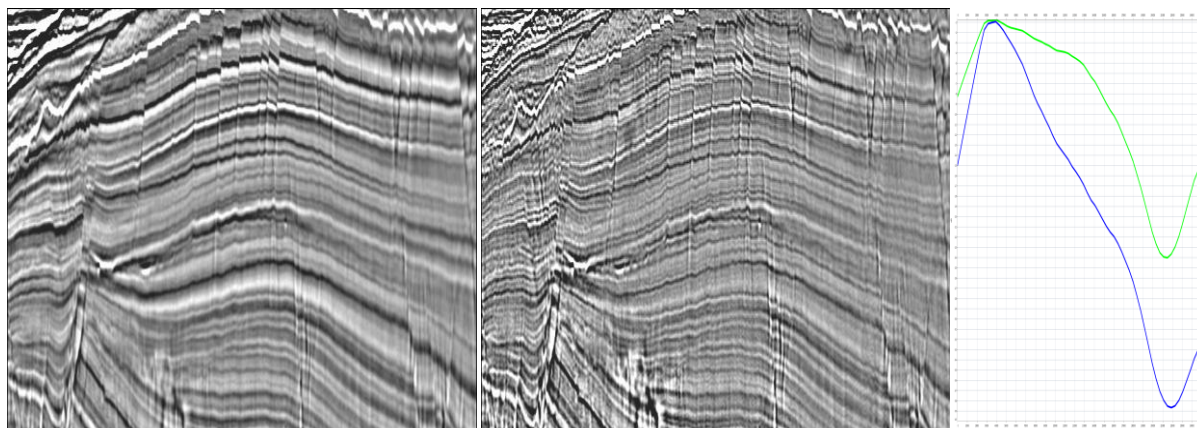


Figure 3 Comparison of vertical sections: the Kirchhoff stack image (left) vs. the least-squares Kirchhoff stack (middle). The right plot shows the spectra, of which the green is least-squares image, and the blue is Kirchhoff. The depth range is 3000 – 4500 m.

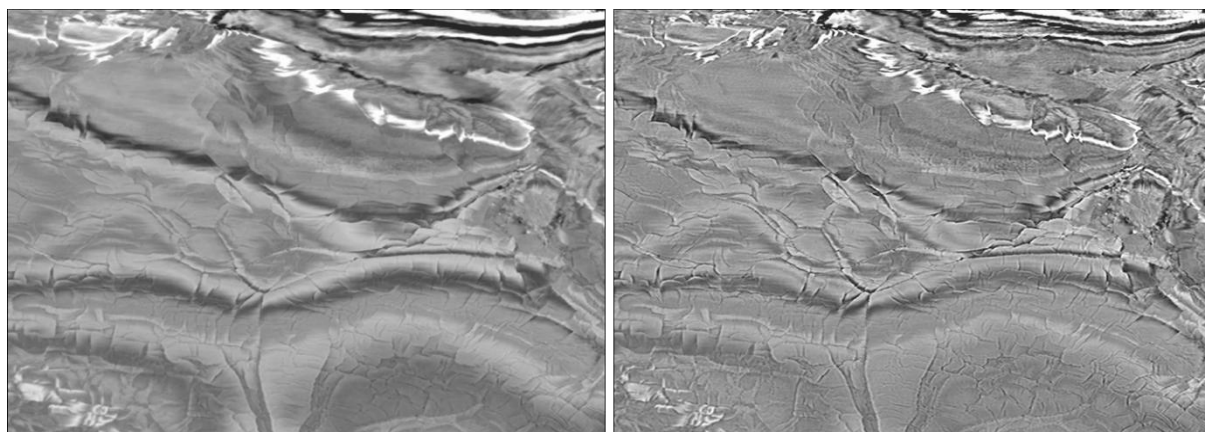


Figure 4 Legacy Kirchhoff stack depth slice (left) and Least-squares Kirchhoff stack depth slice (right) at depth 3100 m.

References

- Albertin, U., Jaramillo, H., Yingst, D., Bloor, R., Chang, W., and Beasley, C., [1999] Aspects of true amplitude migration, SEG Technical Program Expanded Abstracts.
- Fletcher, R. P., Nichols, D., Bloor, R., and Coates, R. T., [2016] Least-square migration – data domain versus image domain using points spread functions, The Leading Edge, February, pp 157–162.
- Lund, H., Purcell, C., and Casasanta, L., [2022] Analytical point spread functions for image domain Least-square Kirchhoff inversion, 83rd EAGE Conference and Exhibition, Extended Abstracts.
- Schuster, J. and Hu, J., [2000] Green's function for migration: Continuous recording geometry, Geophysics, Vol. 65, No. 1, pp 167–175.
- Valenciano, A. and Chemingui, N., [2013] Tomographic Q estimation for viscoacoustic imaging, 75th EAGE Conference and Exhibition, Extended Abstracts.
- Xu, P., Feng, B., Wang, H., and Liu, S., [2022] Noniterative least-squares reverse time migration based on an efficient asymptotic Hessian/point spread function estimation, Geophysics, Vol. 87, No. 4, pp. S169-S184.